Prediction of Sound Pressure Level of Turbulent Noise Generated from Multiple-Disk Fans

by

Yoshio KODAMA*, Hidechito HAYASHI*, Yasuo HAMADA**,
Kiyohiro TANAKA*, Hisato HARAGA*** and Katushi AKAMATSU***

We proposed a theory for estimating the spectral density distribution and over all sound pressure level of the turbulent noise radiated from multiple-disk fans. In the theory, correlations between the longitudinal and lateral correlation lengths, and the pressure spectral densities were used. The effects of casing on the radiated noise were experimentally made clear by comparing the spectral density distributions with and without casing. The validity of theoretically obtained formula was examined with respect to the effects of such parameters as ; the gap between two disks, the rotational frequency, the number of disks, the thickness of disks, the radius of impeller and the flow rate. The agreement between the theoretical and the experimental results was fairly satisfactory.

1. Introduction

Noise generated by fans consists of the discrete frequency noise occuring at the fundamental blade passage frequency and its harmonics, and of the broad band noise extending over a wide range of frequencies. The latter is mostly arising from fluctuating forces in the flow and is called turbulence noise. In a previous paper[1] the authors pointed out that the noise generated by multiple-disk fans (so-called laminar flow fans) is the turbulent noise. There are three mechanisms giving rise to the radiation of the turbulent noise. One is the presence of significiant amounts of turbulence in the oncoming mean flow. The second is the surface pressure fluctuation arising from a turbulent boundary layer developing on a disk. And the third is the shedding of vortex from the trailing edge of a disk.

Of these three mechanisms the noise due to the first one could be ignored if the turbulence in the flow ahead of a blade is weak enough[2]. The second one has been discussed by Fukano et al[3)~5]. and Clark[6]. They pointed out that the turbulent noise due to the vortex shedding from the rotor blade of axial flow fans was greatly influenced by the wake width, and derived a theoretical formula to estimate the sound power. The agreement between the theoretical and experimental results is quite satisfactory, as shown in their papers. Finally on the third mechanism a working formula was theoretically derived for estimating the sound pressure level of turbulent noise, using the spectral densities of surface pressure flulctuation, ϕ_{pp} by Mugridge[7]. The value of ϕ_{pp} was experimentally estimated by measuring the pressure fluctuations on the suction surface of aerofoils which was a major part in comparison with that on the pressure surface. It was shown in his paper that these formulas give fairly good estimations of the noise spectra radiated from a stationary aerofoil in a wind tunnel. We tried to apply his formulas to the multiple-disk fans used in this study but good estimations can not be obtained. Moreover there have been few studies on the prediction of sound

Received at 27-April-1994

* Department of Mechanical Systems Engineering
** Graduate Student, Marine Resources
*** TOTO Ltd.

pressure level of the turbulent noise generated from multiple-disk fans.

In this paper, a theory is introduced to estimate the noise level on the assumption that the noise from multiple-disk fans is mostly turbulent noise. We demonstrated previously that the disk thickness does not influence to the noise level, so this noise is not due to shedding vortices depending on the wake width. The inlet turbulence to the impeller is very small in the absence of any obstacle ahead of the blade. Considering the above, the noise generated from the fans is due to only the surface pressure fluctuation arising from a turbulent boundary layer developing on a disk surface. In this paper we derive to predict the level of turbulent noise radiated from the boundary layer of a disk surface on the assumption that the noise is equally radiated from both sides of the disk surface. Moreover the effects of casing and the parameters of impellers on the noise are experimentally examined. These parameters are: the gap between two disks, the rotational frequency, the number and the thickness of disks, the radius of impeller and the flow rate. By comparing the predicted noise level with the measured noise level, it is made clear that the effects of these parameters on the noise are resonably expressed by the predicted formula.

2. Theory of turbulent noise

2. 1 Sound power radiated from blade surface

Sharland introduced the equation for the sound power of the turbulent noise[2]. The sound power, $dE(\omega)$ per $d\omega$ can be rewritten in next form.

$$dE(\omega)/d\omega=\int_S \omega^2\phi_{pp}S_c dxdy/(12\pi\rho a_0^3) \qquad (1)$$

where E is the sound power radiated from all blades of an impeller, the surface S lies in the x, y plane, ω is the angular frequency, ϕ_{pp} is the spectral density function of the pressure fluctuations on the blade surface, S_c is the correlation area, ρ and a_0 are the density and the sonic velocity of the air respectively.

On the other hand the pressure fluctuations on the blade surface (ϕ_{pp}) was experimentally investigated by Mugridge[7] and the following equation was derived.

$$\phi_{pp}=10^{-3}\rho^2\delta_T^* W^3 \qquad (2)$$

where δ_T^* and W are the boundary layer displacement thickness and mean flow velocity at the trailing edge of the blade.

Another experiment on wall-pressure fluctuations of a flat plate in zero-pressure-gradient was carried by H. H. Schloemer[8]. In his experiment the longitudinal and lateral correlation length were taken to be $8U_c/\omega$ and $1.0U_c/\omega$ respectively, where U_c is the mean convection velocity of boundary layer turbulence and is approximately given by the 0.7 times of mean flow velocity W. Since the correlation area (S_c) in the equation (1) can be written as the products of the longitudinal and lateral correlation length, $S_c=L_xL_y=3.9(W/\omega)^2$.

2. 2 Predicted formula of sound pressure level

The impeller of a multiple-disk fan consists of a stack of closely spaced disks with a central hole for air inlet. Since the noise is transmitted through these closely spaced disks, it may be influenced by the flow condition. But we assume that these influences are negligible. When equation (1) is applied to the multiple-disk fans, the sound power must be estimated by using the pressure fluctuation along the stream line of the mean flow spirally moving from inlet to outlet of the impeller. As showen by Fig. 1 we introduce the radial coordinate r, the coordinate along the flow direction x, the normal to the flow direction y and the angle between the radial coordinate and flow direction β (assumed to be constant). By using the longitudi-

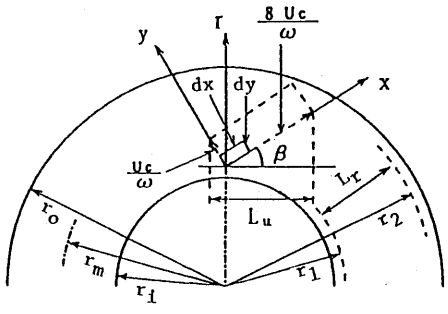

Fig. 1 System of coordinates.

nal and lateral correlation length (L_x and L_y), the correlation length of the radial direction L_r is written by

$$L_r = L_x \sin\beta + L_y \cos\beta = (5.6\sin\beta + 0.7\cos\beta)\, W/\omega \quad (3)$$

To integrate the equation (1), it is convenient to introduce the area $r.\ d\theta.\ dr$ in a system of polar coordinates instead of the area $dxdy$. The noise source equally overspread the annular part of disk surface between r_1 and r_2. Referring to Figure. 1, r_1 and r_2 are given by

$$r_1 = r_m - L_r/2,\ r_2 = r_m + L_r/2 \quad (4)$$

where r_m is the mean radius of the annular spreading noise source. Hence

$$\begin{aligned}\iint S_c dxdy &= \int_0^{2\pi}\int_{r_1}^{r_2} S_c r dr d\theta \\ &= S_c\pi(r_2+r_1)(r_2-r_1) \\ &= 2\pi S_c r_m L_r \\ &= 7.8\pi(W/\omega)^2 r_m(5.6\sin\beta \\ &\quad +0.7\cos\beta)(W/\omega)\end{aligned} \quad (5)$$

Inserting these equations (2), (3), (4) and (5) into the equation (1) and integrating them by ω, one finds the equation (6) as

$$E(\omega) = 6.5\cdot 10^{-4}\rho\delta_T^* r_m(5.6\sin\beta + 0.7\cos\beta)\, W^3 M^3 \int_0^{\omega}(1/\omega)d\omega \quad (6)$$

where M ($= W/a_0$) is Mach number. $E(\omega)$ in equation (6) is the sound power radiated from the annular part of the disk surface between r_1 and r_2. With the definition that δ is the distance between the wall surface and the point of maximum relative velocity W_{max} shown by Fig. 3, the boundary layer displacement thickness δ_T^* was given by

$$\delta_T^* = \int_0^{\delta}(1 - W/W_{max})dz \quad (7)$$

where W is the relative velocity, z is the coordinate perpendicular to the wall surface. The upper limit of integration on equation (6) could be replaced by $\omega = \omega_u$ which is the maximum angular frequency in accordance with the applicable condition ($\omega_u = 2\pi f < 0.6\, W/\delta_T^*$) of equation (2) and the lower limit of that could be replaced by $\omega_\ell = (5.6\sin\beta + 0.7\cos\beta)\, W/(r_0 - r_i)$ which is given by equation (3) with $L_r = r_0 - r_i$. Outside these limits the integrands must be equal to zero. Assumed that the noise sources of disk surfaces are independent of each surface and the noise is equally radiated from both sides of the disk surfaces, the sound power radiated from multiple-disk fans with the number of disks B is given by

$$E(\omega) = KB1.3\cdot 10^{-3}\rho\delta_T^* r_m(5.6\sin\beta + 0.7\cos\beta)\, W^3 M^3 \int_{\omega_\ell}^{\omega_u}(1/\omega)d\omega \quad (8)$$

where K(=constant) represents the effect of casing on the sound radiation. Considering that the source of the noise radiated from a fan is the dipole, the relation between sound pressure (p) and sound power (E) can be written by

$$E/2 = 4\pi Z^2 p^2/(3\rho a_0) \quad (9)$$

where p is measured at distance Z from the noise source on the shaft center of the fan where it is called far field. The sound pressure level SPL at the observation point is given by

$$SPL = 20\log_{10}(p/p_0) \quad (10)$$

where p_0 is the minimum audible sound pressure ($p_0 = 0.00002\mathrm{P_a}$)

2. 3 Relative velocity

The relative velocity is necessary for estimating sound power. Breiter et al[9] derived formula to estimate the radial and tangential composition of relative velocity from momentum equation and equation of continuity. We tried to estimate the sound pressure level using the relative velocity from the formula, and found the process of calculation was very complicated and the agreement between the calculated and experimental results was unsatisfactory. Hence we assumed that the absolute tangential velocity distribution between two disks can be approximated with the fourth power equation as shown in Fig. 2 and equation (11). The equation is given by

$$V_u = az^4 + bz^2 + c \quad (11)$$

where z is the coordinate perpendicular to the disk

surface and its origin is positioned at the center between the two disks and a, b, c are constants. One has the boundary conditions as

$$z=\pm h:\ V_u=ah^4+bh^2+c=r\omega$$
$$z=nh:\ dV_u/dz=4a(nh)^3+2b(nh)=0$$
$$z=h:\ dV_u/dz=4ah^3+2bh=(dV_u/dz)_s$$

where the positions at the minimum velocity (nh) and maximum velocity ($nh=0$) of the absolute velocity profile in tangential component are given by the results of the calculation by Breiter. Using these boundary conditions and arranging the equation (11), V_u is given by

$$V_u=\frac{1}{4h^3(1-n^2)}\left(\frac{dV_u}{dz}\right)_s z^4-\frac{1}{2h(1-n^2)}\left(\frac{dV_u}{dz}\right)_s z^2+r\omega-\frac{(1-2n^2)h}{4(1-n^2)}\left(\frac{dV_u}{dz}\right)_s \quad (12)$$

where ω and $(dV/dz)_s$ are angular disk velocity and velocity gradient normal to the wall at disk surface. The integration of this equation from $z=-h$ to $z=h$ is equal to $\overline{V}_u\cdot 2h$, as shown by the area of the hatching part of Fig. 2. The relation between the average velocity $\overline{V}_u$ and $(dV/dz)_s$ is given by

$$(dV_u/dz)_s=15(1-n^2)(r_\omega-\overline{V}_u)/[(3-5n^2)h] \quad (13)$$

Inserting this equation into the balance equation on the shearing force and momentum[10], and arranging it, now we put $\overline{V}_u$ to $\overline{V}_{uth}$, $\overline{V}_{uth}$ is obtained by

$$\frac{\overline{V}_{uth}}{u}=1-\frac{(3-5n^2)A}{60(1-n^2)\pi}\left(\frac{r_i}{r}\right)+\left\{\frac{(3-5n^2)A}{60(1-n^2)\pi}-1\right\}\left(\frac{r_i}{r}\right)\exp\left[\frac{60(1-n^2)\pi}{(3-5n^2)A}\left\{1-\left(\frac{r}{r_1}\right)^2\right\}\right] \quad (14)$$

where $A(=q/\nu r_i^2)$ is non-dimensional flow rate, q is volume flow rate between two disks and r_i is inner radius of a disk. With the calculating results by Breiter, the value of n is 0 (δ_D=0.7mm), 0.3 (δ_D =1.6 mm) or 0.65 (δ_D=3.0 mm). The authors showed previously that the composition of tangential absolute velocity $\overline{V}_u$ is given by $\overline{V}_u=K_m\overline{V}_{uth}$. K_m is a constant and experimentally obtained by

$$K_m=0.1\frac{L_R}{L_c}\frac{U_o}{a_o}\log_{10}(A_o+1)+\frac{0.78}{e^{\tan\alpha}} \quad (15)$$

where $L_R, L_c, U_o, A_o(=q/\nu r_o^2)$ and α are the axial length of impeller, the path width of casing, the velocity at the outer radius of the disk, the non-dimensional flow rate and the volute angle of the scroll. Since $\overline{V}_{uth}$ is obtained from equation (14) and K_m from equation (15), distribution of V_u between two disks can be calculated from (12) and (13). Hence relative velocity on each radius and flow angle β can be obtained. Fig. 3 illustrates the velocity profiles between two disks and boundary layer thickness δ. As the gap between two disks δ_D decrease, the velocity distribution becomes uniform.

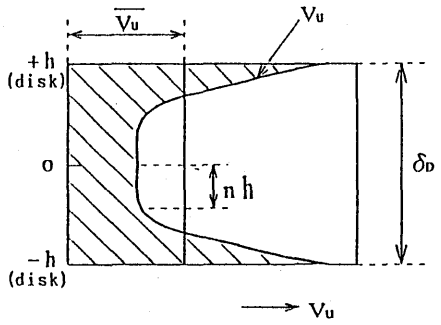

Fig. 2 Absolute velocity profile in tangential component between two disks.

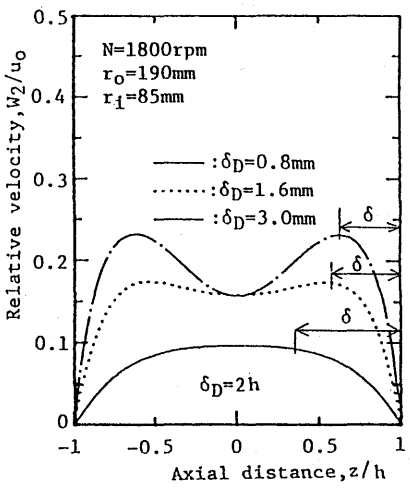

Fig. 3 Velocity profiles between two disks and boundary layer thickness.

3. Experimental Apparatus and Method

The experimental apparatus is shown in Fig. 4, its total length is approximately 2.2m and a test fan is mounted near the suction end of the pipe. In the apparatus, an inlet nozzle and a delivery pipe of length 1.89m were mounted at inlet and outlet of the impeller respectively. Downstream of the fan there is a 1.89m long straight pipe, in which there are an orifice flow meter and a honeycomb which satisfy the Japanese Industrial Standards, and at the exit of the pipe there is a conical damper to adjust the flow rate. The flow was controlled by opening and closing the damper at the pipe outlet. To reduce the noise radiation from the electric motor, the motor was enclosed with a concrete box ceiling with glass wool.

Three impellers were tested. Their outer diameter D_o[mm] and inner diameter D_i[mm] are (380, 170), (310, 130), and (230, 100), respectively. These impellers consist of doughnut-type disks made of aluminium and the thicknesses of disks are 0.8mm, 1.5mm and 3.0mm. Three kinds of casing were also tested corresponding to the three impellers and their volute angle of scroll is all 7°. The radius at the cutoff position of the casing R_c are 210, 185 and 140mm and these casings are called Casing A, B, and C, respectively. Another volute angle of scroll 2° and 4° were also prepaired and the effects of the casing on noise were examined. Moreover three kinds of the number of disks B=10, 20 and 30 and three kinds of the distance between disks δ_D=0.8, 1.5 and 3.0mm were tested. Since we found that a thinner disk can make fan efficiency higher, the thickness of the disk D_t=0.8mm were mainly used and D_t=1.6 and 3.0mm were also tested in this paper. The noise level was measured at 1m upstream from the inlet nozzle on the shaft center of the fan. Frequency analysis of the output from the noise level meter was made by an FFT analyzer and recorded with a high speed recorder. The resolution of FFT analyzer used in this test was about 20 Hz.

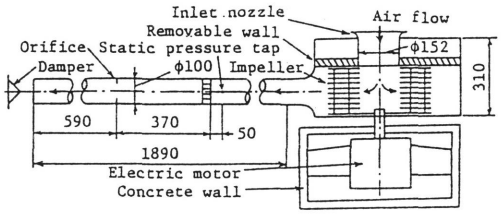

Fig. 4 Schematic diagram of experimental apparatus (Dimmensions in mm).

4. Experimental Results and Discussions

4. 1 Aerodynamic characteristics of fans

Examples of the characteristic curve of the fan are presented in Fig. 7. In the figure, ψ, ϕ and η are the pressure coefficient, the flow coefficient and the combined efficiency of the motor and the fan[1]. The total pressure efficiency and pressure coefficient are decreased with decreasing outer radius of the impeller. This result was explained by the following two reasons: One reason is that as the outer radius of the impeller is decreased, the clearance between the casing wall and the back shroud must be increased relatively from the manufacturing point of view so that the mixing loss at the outlet of the impeller is increased. The second reasons is that the ratio of inlet length to the length

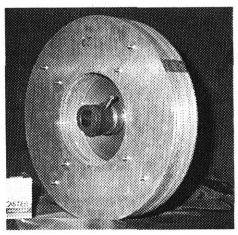

Fig. 5 Impeller used in this experiment.

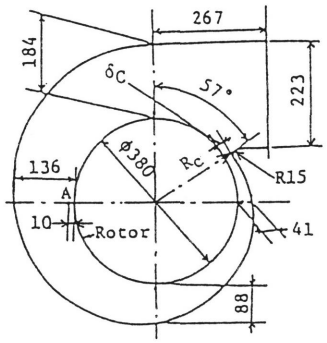

Fig. 6 Casing used in this experiment (Casing A).

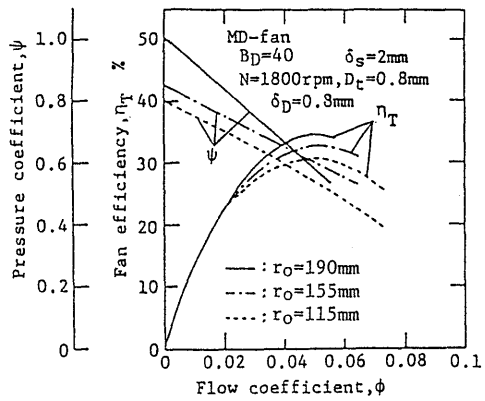

Fig. 7 Characteristic curve. ψ, ϕ and η_T are pressure coefficient, flow coefficient and combined efficiency of the motor and fan, respectively.

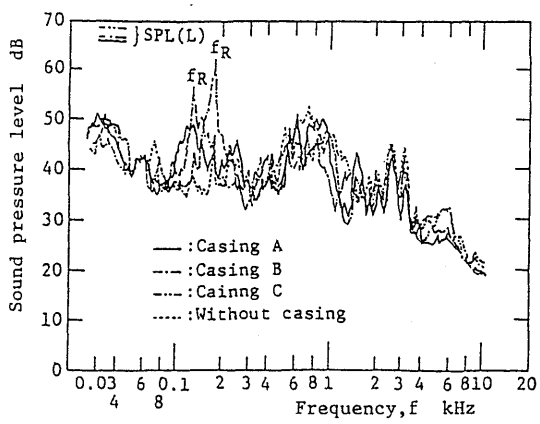

Fig. 8 Effect of casing on spectral density distribution. The solid line, broken line, one-dot chain line and two-dot chain line indicate the data corresponding respectively to the casing A, casing B, casing C and without casing.

from inlet to outlet of the impeller is increased with the decrease in the outer radius of the impeller so that the ratio of the frictional loss on this region to the total loss is increased.

4. 2 Acoustic characteristics of casing

The effect of the size of the casing on the sound radiation was examined as below. The sound was radiated from a speaker (240mm in diameter). The sound radiation from the speaker mounted at the center of the casing was measured. Fig. 8 shows the effect of casing on sound radiation. The discrete frequency sound in the range of 100 ~ 200Hz is generated but this sound is not generated in the case of without casing. As the size of the casing comes to smaller, the discrete frequency f_R shown in Fig. 8 changes in higher and the sound pressure level at the frequency f_R is increased. These increase and decrease of the speaker sound are due to the difference of the resonance frequency of the casing. The discrete frequency spectrum except for the resonance sound and the broad band frequency spectrum in the range of 0.6 ~ 1kHz are due to the speaker characteristics since these noises are independent of the presence of casing and of the variations of casing. Hence the effect of casing on speaker sound is appeared only at the resonance frequency.

Moreover, comparison of the over-all level of the speaker sounds measured by the noise level meter without any filters (L characteristic) shows that the effect of casing is decreased with the increasing casing size. Using the over all sound power level with the casing, K(=constant) introduced in equation (8) can be calculated, and K of casing A, B and C are 0.95, 1.0, and 1.2, respectively. Now if the deduction value of the resonance sound power level from the over-all one is used in place of the over-all level, K is calculated to be nearly 1 unrelated to the size of the casing. Since the main purpose of this study is the prediction of turbulent noise level instead of resonance noise level, $K=1$ is used on the following calculation of the over-all sound pressure level. When the resonance noise is generated in test, we deducted the resonance sound power level from over-all noise level and used this value as the experimental results of over-all turbulent noise for the purpose of compairing experimental and thoretical results.

4. 3 Comparison between calculated and measured results

4. 3. 1 An aspect of flow

The relative velocity at impeller outlet was measured at four circumferential sections 90 degree apart (A, B, C and D as shown by Fig. 6) and ten axial locations at each section. Fig. 9 shows the axial distance versus relative velocity of measured

and calculated results with volute angle of the scroll α. The agreement between the measured and calculated results is quite satisfactory. As α increased, the relative velocity increased. This could be explained by that, K_m decreases and tangential velocity increases with increasing α.

Fig. 10 shows the effect of the various gaps of two disks δ_D and impeller rotational frequency on the calculated displacement thickness δ_T^*. It is found that the value of δ_T^* is increased with decreasing the rotational frequency and with increasing δ_D.

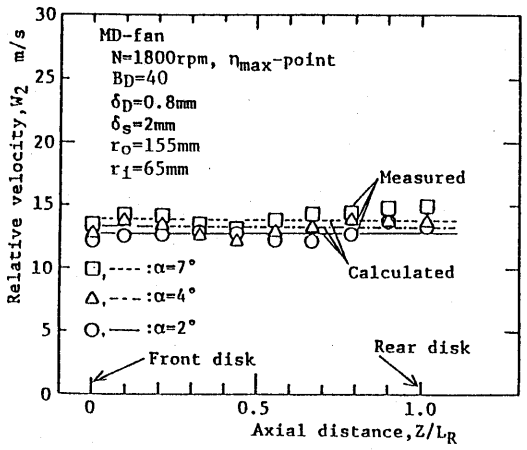

Fig. 9 Axial distance versus relative velocity of measured and calculated results with volute angle of the scroll α.

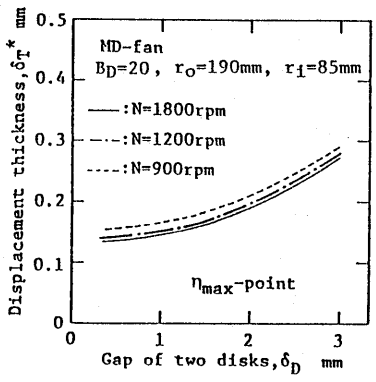

Fig. 10 Effect of gap between two disks on displacement thickness.

4. 3. 2 Spectral density distribution of fan noise

Both calculated and measured spectrum density of fan noise by using the casing A, B and C are shown in Fig. 11 (a), (b), and (c), respectively. The relative velocity W and relative flow angle β vary with its radial location between the inlet and outlet of the impeller. Considering that the sound power is in proportion to the 6th power of the velocity averaged by inlet and outlet of the impeller, the value of W and β at mean radius are used on calculating the sound power level. If the flow rate and rotational frequency are given, the radial veloc-

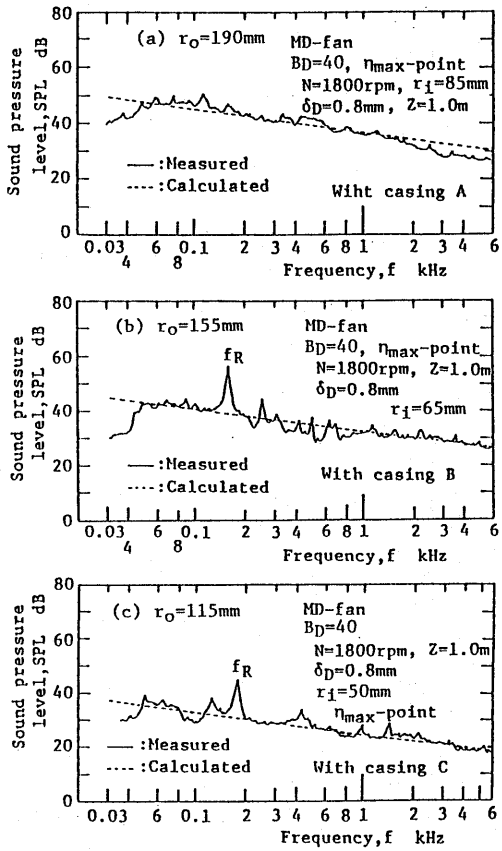

Fig. 11 Spectrum density distribution of fan noise. The solid line and dotted-line show the measured and calculated results respectively. The calculation of sound pressure level is made by 20Hz band width. B, N, r_o, r_i and δ_D are the number of disks, rotational frequency, outer and inner radius of the impeller and the gap of two disks respectively.

ity V_a and disk velocity u at mean radius are calculated, and $\overline{V}_u$ is calculated using equation (14) and (15), so that the relative velocity W and the relative flow angle β are obtained by velocity triangle. The agreement between the measured and calculated results is fairly good in the frequency range of 0.06~1kHz.

If the correction of the effect of the casing is done in each frequency band width, it is expected that better agreement will be obtained. The discrete frequency noises in the frequency range of 0.1 ~0.2kHz shown in Fig. 11 (b) and (c) are supposed to be resonance noise. These noises are due to the resonance between the casing and the turbulence on internal flow of the fan as shown in Fig. 8. Compairing the noise spectral density in Fig. 11 (a), (b) and (c), it comes to be clear that increasing the sound pressure level at over-all range of frequency, increasing the impeller diameter. The reason is that as the impeller diameter is large, the tangential velocity and flow rate are increased and the relative velocity is increased. According to equation (8), the relative velocity is one of the most important parameters influencing the noise level.

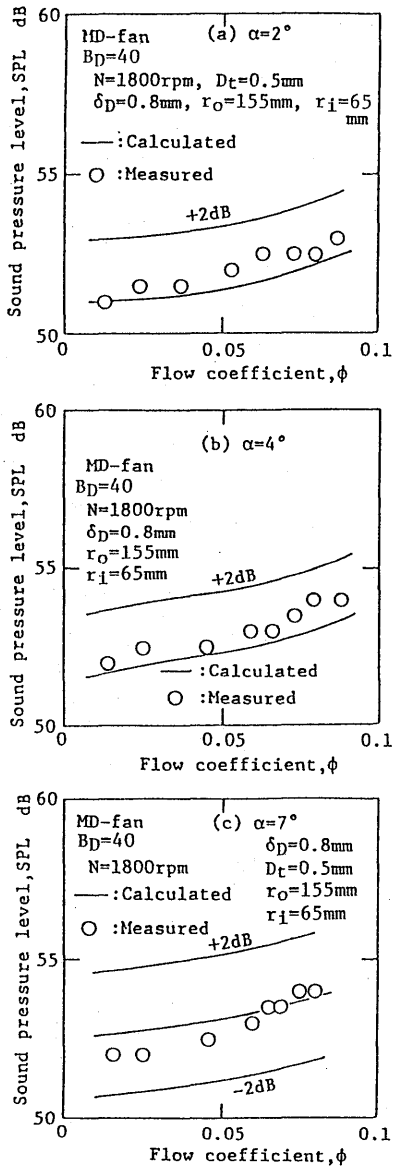

Fig. 12 Effect of flow coefficient on over all noise level.

4. 3. 3 Effects of flow rate on fan noise

Fig. 12 (a), (b) and (c) show the relationship between flow coefficient and over-all sound pressure level with the volute angle of scroll α=2°, 4° and 7° respectively, where rotational frequency N is 1800rpm. The agreement between the measured value marked by ○ and calculated value marked by solid line is fairly good. The sound pressure level increases with the increase in α because of the increase in relative velocity that greatly influences to the sound pressure level. By the same reason the sound pressure level increases with increasing

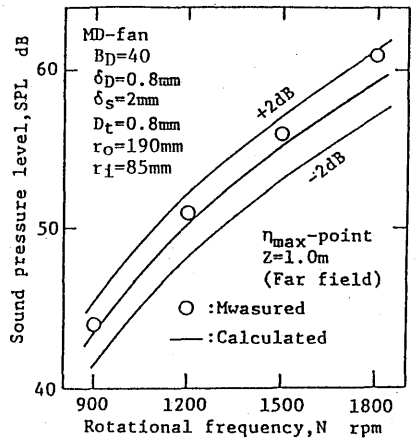

Fig. 13 Effect of rotational frequency on over all noise level. The symbol ○, thick solid line and thin solid line indicate the measured value, calculated value and its error range of ± 2dB respectively. The number of disks is 40.

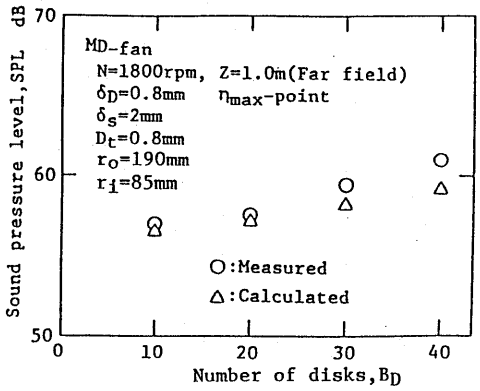

Fig. 14 Effects of the number of disks on sound pressure level. The symbol ○ and △ indicate measured and calculated value respectively. The gap between every two disks is 0.8mm.

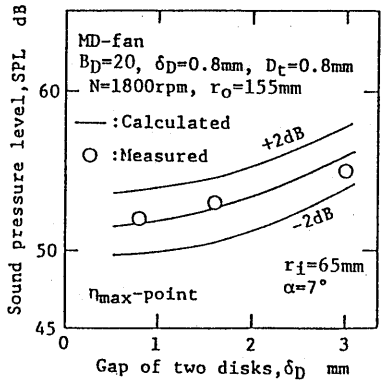

Fig. 15 Relationship between the gap of disks and sound pressure level with casing A. The symbol ○ and thick solid line indicate measured and calculated value respectively.

flow rate.

4. 3. 4 Effects of rotational frequency

Fig. 13 shows the effects of rotational frequency on sound pressure level. Rotational frequency influences to the relative velocity and therefore the sound pressure level. As shown in this figure its influence is fairly great. The measured value can be predicted by the equation derived in this paper with a sufficient accuracy within ± 2dB.

Fig. 14 shows the effects of the number of disks on sound pressure level. Doubling the number of disks, the sound pressure level becomes 3dB up.

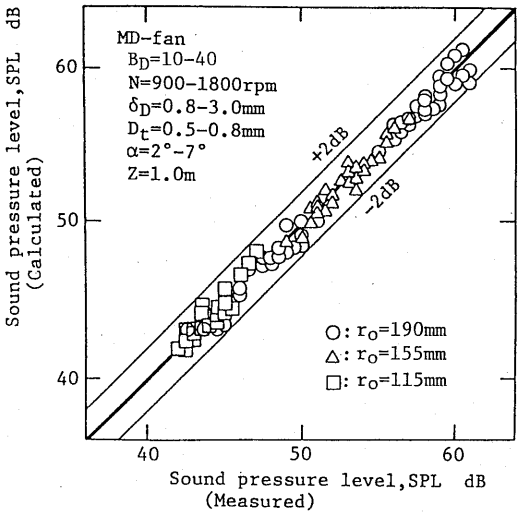

Fig. 16 Comparison between the measured and calculated value of sound pressure level.

This demonstrates that the sound source of each disk is independent from other sources as assumed in equation (8).

Fig. 15 shows the relationship between the gap of disks and the noise generated from the fan. The sound pressure level increase with the increase in δ_D because of the increase in relative velocity.

Fig. 16 shows the comparison between the measured and calculated value of sound pressure level with various kinds of parameters on three impellers which has different outer radius. The outer radius of three impellers are 190mm (marked by ○), 155mm (△) and 115mm (□). The data for the impellers of outer radius 150mm and 115mm with rotational frequency of 1200rpm and 900rpm are excluded in this figure because the difference between the radiating noise and back ground noise level is so little that the agreement between the measured and calculated value is bad.

The plots which fall just on the thick solid line in Fig. 16 signify that the experimental values are well agreement with the theoretical values and scatter within the error range of ± 2dB shown by thin solid lines. According to these results it is evident that formula (8) is valid in estimating sound pressure level for the wide variation in the number of disks, the gap of disks, rotational frequency, spiral extension index of scroll and flow rate.

5. Conclusion

Theoretical and experimental investigations are performed to make clear the effects of casing and a number of parameters; the gap between two disks, the rotational frequency, the number of disks, the thickness of disk, the radius of the impeller and the flow rate. The validity of thoretically obtained formula was examined. The results are as follows.

(1) For the wide variation of parameters affecting the turbulent noise which is generated from the multiple-disk fans, the over-all turbulence noise level can be predicted by the equation (8) with a sufficient accuracy within ± 2dB in this experiment.

(2) The sound power level of noise radiation is influenced by casing over-all frequency. In oder to predict the noise level with good accuracy, it is neccesary to consider the effect of the casing in general. But in this experiment the agreement between the measured and calculated results are fairly good without the considering the effect. On designing the fans it is neccesary to be careful of the resonance sometimes occuring between the casing and turbulence of the flow in the impeller.

(3) As the volute angle of the scroll increases, the relative velocity increases and then the noise level increases.

(4) As the gap between two disks increases, the relative velocity and displacement thickness increase and therefore the noise level increases.

(5) The increase of the flow coefficient results the increase in the relative velocity and noise level.

REFERENCES

1) Y. Kodama, et al., Transactions of the Japan Sosiety of Mechanical Engineers 58-549, (1992), 1611.
2) Sharland, I. J., Sound Vib., 1-3, (1964), 302.
3) T. Fukano, et al., Transactions of the Japan Sosiety of Mechanical Engineers 41-345, (1975), 1479.
4) T. Fukano, et al., Transactions of the Japan Sosiety of Mechanical Engineers 43-375, (1977), 4168.
5) T. Fukano, et al., Transactions of the Japan Sosiety of Mechanical Engineers 51-463, (1985), 820.
6) Clark, L. T., et al. J. Acous. Am. 59-1, (1976), 24.
7) Mugridge, B. D. J. Sound Vib. 16-4, (1971), 593.
8) Schloemer, H. H. J. Acous. Am. 42-1, (1967), 93.
9) Breiter, C. and Pohlhausen, K. A. R. L. Rep. No. ARL, (1962), 62-318.
10) Hasinger, S. and Kehrt, L. Trans. ASME, J. Eng. power 85, (1963), 201.

APPENDIX

Nomenclature

a_o : sonic velocity of air, m/s
B_D : number of disks
D_t : thickness of disk
E : sound power, W
f : frequency, Hz
f_R : resonance frequency, Hz
g : acceleration of gravity, m/s^2
H : total pressure rise, mmAq or mAir
N : rotational frequency, rpm
p : pressure fluctuation, Pa
p : sound pressure, Pa
p_o : minimum audible sound pressure, Pa
Q : flow rate of fan, m^3/s or m^3/min
r_o : outer radius of impeller, mm or m
r_i : inner radius of impeller, mm or m
r : radius on disk, mm or m
S_c : correlation area, mm^2 or m^2
SPL: sound pressure level, dB
t : time, s
U_c : mean convection velocity, m/s
u_o : disk velocity at outer radius, m/s
W : relative velocity, m/s
Z : Distance between measuring point and noise source, m
z : Coordinate perpendicular to the disk surface, m or mm
α : volute angle of scroll, degree
β : flow angle, degree
δ : boundary-layer thickness, mm or m
δ_D : distance between disks, mm or m
δ_T : boundary-layer displacement thickness, mm or m
η_T : total pressure efficiency
λ : inlet power coefficient
ν : kinematic viscosity of air, m^2/s

ρ : air density, kg/m^3

ϕ : flow coefficient

ϕ_{PP} : spectral density function of pressure fluctuation

ψ : pressure coefficient

ω : angular disk velocity, rad/s